Appl. Phys. A 84, 203–206 (2006)
DOI: 10.1007/s00339-006-3601-5

Applied Physics A
Materials Science & Processing

F. KONG[1]
X.L. WU[1,✉]
G.S. HUANG[1]
R.K. YUAN[1]
C.Z. YANG[2]
P.K. CHU[3]
G.G. SIU[3]

Temperature-dependent photoluminescence from MEH-PPV and MEH-OPPV containing oxadiazole in the main chain

[1] National Laboratory of Solid State Microstructures and Department of Physics, Nanjing University, Nanjing 210093, P.R. China
[2] College of Chemistry and Chemical Engineering, Nanjing University, Nanjing 210093, P.R. China
[3] Department of Physics and Materials Science, City University of Hong Kong, Kowloon, Hong Kong, P.R. China

Received: 26 January 2006/Accepted: 24 March 2006
Published online: 26 April 2006 •

ABSTRACT We report the temperature-dependent photoluminescence (PL) behavior of two poly (*p*-phenylene-vinylene) derivatives with different backbones, a homopolymer poly-[2-methoxy-5-(2′-ethyl-hexyloxy)-1,4-phenylene-vinylene] (MEH-PPV) and a copolymer poly-{[2-methoxy-5-(2-ethyl-hexyloxy)-1,4-phenylene-vinylene]-alt-[2,5-diphenylene-1,3,4-oxadiazole-vinylene]} (MEH-OPPV). The PL peak positions of the MEH-PPV in both solid solution and film are blue shifted with increasing measurement temperature because the thermally induced torsion and libration modes reduce the conjugation lengths of the polymer, but the shift rate is smaller in the MEH-PPV film than that in the solid solution. The PL peak position of the MEH-OPPV film is independent of measurement temperature because there is a large dihedral angle between the adjacent monomer units. The large dihedral angle increases the conformational disorder to eliminate the effect of the disorder induced by the thermally induced torsion and libration modes on the conjugation lengths of the MEH-OPPV.

PACS 73.61.Ph; 78.55.Kz

The electrical and optical properties of conjugated polymers, especially poly (*p*-phenylene-vinylene) (PPV) and its derivatives, have been studied extensively for both fundamental photophysics and applications in optoelectronic devices, such as light-emitting diodes, solid-state lasers, solar cells, and biological sensors [1–5]. Because photoluminescence (PL) from PPV and its derivatives is critical in many applications, it is important to establish a correlation between polymer structures and fundamental photophysics, such as excitation generation, excitation energy transfer, and recombination. The temperature dependence and photophysical studies can provide valuable information about the absorption and emission characteristics of conjugated polymers [6–10]. For instance, temperature-dependent single-molecule spectroscopy studies can yield more insights into the energy-transfer process in conjugated polymers [11, 12].

In this paper, we present the temperature-dependent PL spectra of a homopolymer poly-[2-methoxy-5-(2′-ethyl-hexyloxy)-1,4-phenylene-vinylene] (MEH-PPV) and a copolymer poly-{[2-methoxy-5-(2-ethylhexyloxy)-1,4-phenylene-vinylene]-alt-[2,5-diphenylene-1,3,4-oxadiazole-vinylene] (MEH-OPPV) containing aryl-substituted oxadiazole groups in the backbone. The PL peak positions of the MEH-PPV in solid solution and film show a blue shift with increasing measurement temperature. Different from the PL property of the MEH-PPV, the PL peak positions of the MEH-OPPV in a form of film are independent of measurement temperature ranging from 80 to 290 K. By analyzing the lowest-energy conformations of the conjugated polymers, it is believed that the large dihedral angle between the adjacent units eliminates the effect of the thermally induced torsion and libration modes on the conjugation lengths of the copolymer, which leads to a thermal stability of the PL peak positions.

The MEH-PPV and MEH-OPPV were synthesized via a modified Glich-polymerization procedure and a Wittig condensation reaction, respectively. The detailed polymerization processes have been reported in our previous work [13, 14]. The chemical structures of the PPV derivatives are shown in Fig. 1a. The mass average molecular weight (M_w) was measured by gel permeation chromatography (GPC) to be 5×10^5 g/mol for the MEH-PPV and 16 400 g/mol for the MEH-OPPV. Figure 1b shows the stereo depictions of the lowest-energy conformations of the PPV derivatives, generated by employing a conformational search using an MM2 force field as implemented in ChemDraw Ultra 7.0. In the preparation of the polymer films, the MEH-PPV and MEH-OPPV were dissolved in tetrahydrofuran (THF) to form solutions with a final concentration of 2 mg/ml. The films were prepared by drop coating the solutions on quartz substrates. Polystyrene was dissolved in a diluted MEH-PPV solution with the ratio of MEH-PPV to polystyrene by weight being 1/1000. The blend solution was drop coated on a quartz substrate to yield a solid solution after the solvent volatilized completely.

The PL spectra of the samples were measured on a T64000 triple Raman system of Jobin Yvon Company, using the 488-nm line of an Ar^+ laser as excitation source. The samples were mounted in a nitrogen-flow cryostat cooled to a temperature of 80 K. The PL spectra were collected from the front of the samples using a backscattering configuration.

Figure 2 shows the PL spectra of the MEH-PPV in solid solution measured at temperatures ranging from 80 to 290 K. There are two obvious vibronic peaks in each PL spectrum,

✉ Fax: +86-25-83595535, E-mail: hkxlwu@nju.edu.cn

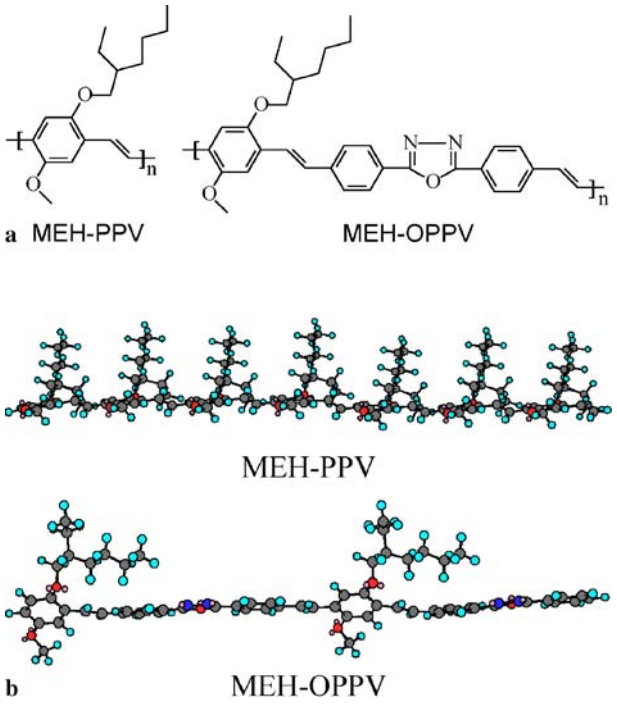

FIGURE 1 (**a**) Chemical structures of the MEH-PPV and MEH-OPPV, (**b**) stereo depictions of the lowest-energy conformations of the MEH-PPV with seven repeat units and the MEH-OPPV with two repeat units

a main peak and a shoulder, which are well resolved at low measurement temperature. The energy difference between them is 0.16 eV. It is nearly independent of temperature and indicative of the coupling of carbon–carbon stretch libration to the conjugated backbone [10]. The intensities of the PL spectra of the MEH-PPV in solid solution decrease and the peak positions blue shift with increasing temperature. The inset in Fig. 2 shows the energy positions of the main and shoulder peaks as a function of temperature. (The peak positions are determined by three-peak Gaussian fitting. We found that the third PL peak with the lowest energy is too weak to be discussed more.) The values of the shift rates for the main and shoulder peaks are $5.1 \times 10^{-4} \pm 0.2$ and $5.6 \times 10^{-4} \pm 0.2$ eV/K, respectively. It has widely been accepted that the conformational disorder disrupts the conjugation of conjugated polymers due to torsion and libration motions [15–17]. Conjugated polymers can be regarded as an inhomogeneous integration of segments with different conjugation lengths and hence have different excitation energies, each of which has a corresponding unbroken π-system. The optical properties of conjugated polymers are related to the conjugation segment length. The experimental results and some calculations have indicated that the energies of the torsion and libration modes of the PPV backbone range between 8.5 and 84 meV [18]. The thermally induced torsion and libration modes increase the conformation disorders to shorten the conjugation segments in the MEH-PPV with increasing temperature and thus reduce the extent of π-electron delocalization and increase the energy of the π–π^* transition. As a result, a blue shift occurs in the PL spectra of the MEH-PPV in solid solution at high temperature.

The PL spectra of the MEH-PPV in film measured under different temperatures are plotted in Fig. 3. The PL band of the MEH-PPV in film is red shifted markedly compared to that in solid solution at the same temperature because of the aggregation of the conjugated polymer chains in the film. The PL spectrum of the MEH-PPV in film contains a main peak and a shoulder, which are also resolved better at lower temperature. Recently, our experiments have shown that the main peak in the MEH-PPV film is connected with the aggregation of the conjugation segments [19]. However, the origin of the shoulder is still unclear. Some research groups infer that the shoulder may be related to the interchain species due to its long PL decay time [20]. From Fig. 3, it can be seen that the shoulder position blue shifts with increasing measurement temperature. A similar blue shift of the PL peak with temperature for the MEH-PPV film has previously been observed by other research groups [6–8]. As discussed above, the increase of the thermally induced torsion and libration modes contributes to the blue shift. The energy position of the PL peak as a function of temperature is plotted in the inset of Fig. 3 (the peak positions are also from three-peak Gaussian fitting). The shift rate of the main PL peak in the MEH-PPV film is $2.6 \times 10^{-4} \pm 0.1$ eV/K and is nearly half of the value observed in the MEH-PPV solid solution. The MEH-PPV chains are separated by polystyrene in solid solution and the interchain interaction between the MEH-PPV chains can be ignored. The MEH-PPV chains can aggregate with π-stacks in the film, in which the strong interchain interactions affect the electrical and optical properties of the MEH-PPV film. In this case, ro-

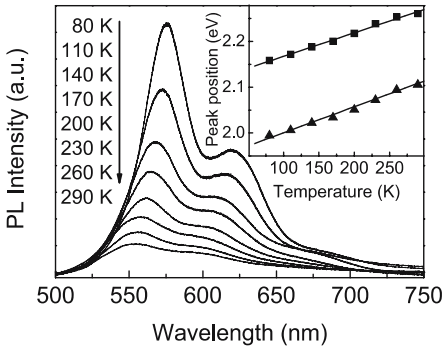

FIGURE 2 PL spectra of the MEH-PPV in solid solution measured under different temperatures. The *inset* shows the energy positions of the main peak (■) and the shoulder peak (▲) as a function of temperature in the MEH-PPV solid solution

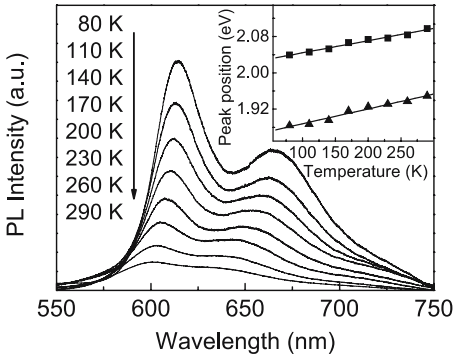

FIGURE 3 PL spectra of the MEH-PPV in film measured under different temperatures. The *inset* shows the energy positions of the main peak (■) and the shoulder peak (▲) as a function of temperature in the MEH-PPV film

tations around the single bonds in the conjugated chains must overcome the conformational barrier and the interchain interaction between the conjugated polymer chains. Thus, some of the rotation modes are restricted in the MEH-PPV film. As a result, the conjugation lengths of MEH-PPV in the film are reduced more slowly than in the solid solution with increasing temperature.

Moreover, it can also be seen from Figs. 2 and 3 that the intensity of the shoulder peak goes up compared to the main peak with increasing temperature. As a conjugation segment in the MEH-PPV is photo-excited by the 488-nm line of an Ar^+laser, the excited excitons will migrate to low-energy sites via Förster energy transfer until they are trapped at the lowest-energy sites, where emission occurs [12, 21, 22]. Based on Förster theory, the energy transfer depends on spectral overlap between donor and acceptor. At higher temperature, the thermally induced disorder in the MEH-PPV results in broader spectral widths causing a larger spectral overlap, which facilitates the excitation energy transfer in conjugated polymers [12]. As a result, there are more excitons for emission at the shoulder peak position with increasing temperature. From the above result, we can obtain information about electron–phonon coupling. The electron–phonon coupling strength in a molecule can be described by the Huang–Rhys factor, S [23]. The S value can be determined by calculating the shoulder PL peak (1–0 transition) intensity relative to the main PL peak (0–0 transition) intensity: $S = I_{1-0}/I_{0-0}$. In the PL spectra of the MEH-PPV, the relative intensity of the shoulder increases in the sample with increasing temperature. This implies the increase of the S value, indicating that the average number of phonons increases when the excited molecule relaxes from its ground-state configuration to a new equilibrium in the excited state.

Figure 4 displays the PL spectra in the MEH-OPPV film measured under different temperatures. Different from MEH-PPV, the PL peak position of the MEH-OPPV film does not shift obviously for temperatures ranging from 80 to 290 K. The MEH-OPPV consists of two kinds of monomer units, a 2-methoxy-5-(2′-ethyl-hexyloxy)-phenylene-vinylene (MEH-PV) unit and an aryl-substituted oxadiazole unit, which are covalently bonded with each other. The two adjacent monomer units have different symmetries and orbital energies, which reduces the electron coupling [24]. Figure 1b shows the lowest-energy conformations of the MEH-PPV with seven repeat units and the MEH-OPPV with two repeat units. All the monomer units are nearly coplanar in the MEH-PPV, in which the electronic coupling is maximal between adjacent monomer units [25]. However, the aryl-substituted oxadiazole groups introduced into the polymer backbone destroy the planar conformation. There is approximately a 35° dihedral angle between the planes of the two adjacent monomer units in the MEH-OPPV due to the conjugation between the nitrogen lone pair electrons and the π-electrons [26]. The π-electron delocalization along the MEH-OPPV chain is restricted by the nonplanar conformation caused by rotation along the C–C bond joining MEH-PPV and aryl-substituted oxadiazole units. The electronic coupling between adjacent monomer units in a conjugated polymer chain strongly depends on the dihedral angle. The large dihedral angle increases the conformational disorder of the MEH-OPPV. The strong disorder disrupts the conjugation, so that the MEH-OPPV becomes a connected system of shorter-length conjugated units than the MEH-PPV [27]. The excitons created in the MEH-OPPV by photo-excitation will be confined in a short conjugation segment. As a result, the PL peak position of the MEH-OPPV is blue shifted relative to that of the MEH-PPV. The effect of the conformational disorder on the optical properties of the MEH-OPPV is mainly attributed to the large dihedral angle between adjacent monomer units. In addition, we notice that there is a low high-energy shoulder at ~ 510 nm in the PL spectrum of the MEH-OPPV film at 80 K. The energy difference between the shoulder and main peaks is about 0.14 eV, slightly smaller than that observed in the MEH-PPV. The widths of the shoulder and main PL peaks are widened due to an increase of conformational disorder caused by the ring torsions [7]. As a result, they gradually overlap with increasing temperature. Finally, the shoulder becomes unidentified.

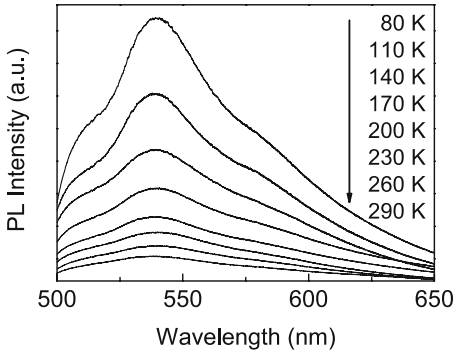

FIGURE 4 PL spectra of the MEH-OPPV in film measured under different temperatures

It was known that as the measurement temperature increases, the conduction and valence bands of semiconducting polymers are expected to be renormalized by electron–phonon interaction and volume expansion associated with C–C bond librations. The decrease of the energy gap is related to the Bose–Einstein statistical factors for phonon emission plus absorption [10]:

$$E_g(T) = E(0) - \frac{2a}{\exp(\Theta/T) - 1}, \tag{1}$$

where $E(0)$ is the band-gap energy at 0 K, a the strength of the exciton–phonon interaction including contributions from both the acoustic and optical phonons, and Θ the average phonon temperature.

In the MEH-OPPV, the large dihedral angle in the backbone limits π-electron delocalization and exciton migration. Therefore, excitons are localized near the sites where the conjugation segments are photo-excited. In this case, the emission spectra from the MEH-OPPV depend on the change of the band gaps of the excited conjugation segments. Narrowing of the energy band width increases the band gap since some of the torsion and libration modes are frozen out at low temperature. The increase of the band gap in the MEH-OPPV film is comparable with its decrease with temperature due to the electron–phonon interaction. As a result, the PL peak position

of the MEH-OPPV film is independent of measurement temperature. Different from the MEH-OPPV, the MEH-PPV has a planar conformation. Excitons can easily migrate from high-energy sites to low-energy sites. The increased conjugation of the MEH-PPV with decreasing temperature contributes to the red shift of the PL peak because the exciton migration plays a dominant role.

We can see from all the PL spectra that the intensities of the PL spectra of the PPV derivatives increase at low temperature. This behavior is related to an increase in the PL quantum yield depending on the relative rates of radiative and nonradiative decay [28]. Freezing out the thermally induced torsions and librations lowers the probability of energy transfer and the radiative decay becomes a dominant process for exciton relaxation in the PPV derivatives. It therefore leads to an increase in the PL quantum yield.

We can also see that the bandwidths of the main PL bands of the PPV derivatives are broadened at high temperature. An increased trend of the PL bandwidth with increasing temperature in the two kinds of PPV derivatives with a planar backbone (MEH-PPV) and a nonplanar backbone (MEH-OPPV) confirms that the temperature-dependent PL bandwidth is due to thermally induced disorder, thereby contributing to a homogeneous broadening. Homogeneous broadening mainly derives from low-frequency librations (i.e. internal torsional modes) in fluorescent molecules [29]. The thermal energy in the low-frequency libration becomes comparable to the intramolecular relaxation energy at high temperature, which gives rise to broadening of the steady-state PL band [30, 31].

In conclusion, we have presented the temperature-dependent steady-state PL spectra from the PPV derivatives with different backbones. The MEH-PPV shows a blue-shifted PL peak in both solid solution and film with increasing temperature. The shift rate of the PL peak in the MEH-PPV film is smaller than that in the solid solution because the aggregation of the polymer chains restricts the thermally induced torsion and libration modes. The MEH-OPPV with a low degree of conjugation shows a PL peak position independent of temperature, because the large dihedral angle between the adjacent monomer units eliminates the effect of the disorder caused by the thermally induced torsion and libration modes on the conjugation lengths with increasing temperature. The temperature-dependent PL bandwidth in the PPV derivatives is due to homogeneous broadening caused by thermally induced disorder.

ACKNOWLEDGEMENTS This work was supported by Grant No. 10225416 from the National Natural Science Foundations of China and the LAPEM. Partial support was also received from Jiangsu Planned Projects for Postdoctoral Research Funds, the Major State Basic Research Project No. G001CB3095 of China, and the City University of Hong Kong Direct Allocation Grant No. 9360110.

REFERENCES

1 R.H. Friend, R.W. Gymer, A.B. Holmes, J.H. Burroughes, R.N. Marks, C. Taliani, D.D.C. Bradley, D.A.D. Santos, J.L. Bredas, M. Logdlund, W.R. Salaneck, Nature **397**, 121 (1999)
2 M.D. McGehee, A.J. Heeger, Adv. Mater. **12**, 1655 (2000)
3 D.T. McQuade, A.E. Pullen, T.M. Swager, Chem. Rev. **100**, 2537 (2000)
4 A.J. Heeger, J. Phys. Chem. B **105**, 8475 (2001)
5 C.J. Brabec, N.S. Sariciftci, J.C. Hummelen, Adv. Funct. Mater. **11**, 15 (2001)
6 T.W. Hagler, K. Pakbaz, K.F. Voss, A.J. Heeger, Phys. Rev. B **44**, 8652 (1991)
7 N.T. Harrison, D.R. Baigent, I.D.W. Samuel, R.H. Friend, A.C. Grimsdale, S.C. Moratti, A.B. Holmes, Phys. Rev. B **53**, 15 815 (1996)
8 A.K. Sherdian, J.M. Lupton, I.D.W. Samuel, D.D.C. Bradley, Chem. Phys. Lett. **322**, 51 (2000)
9 F.A.C. Oliveira, L.A. Cury, A. Righi, R.L. Moreira, P.S.S. Guimarães, F.M. Matinaga, M.A. Pimenta, R.A. Nogueira, J. Chem. Phys. **119**, 9777 (2003)
10 S. Guha, J.D. Rice, Y.T. Yau, C.M. Martin, M. Chandrasekhar, H.R. Chandrasekhar, R. Guentner, P. Scanduicci de Freitas, U. Scherf, Phys. Rev. B **67**, 125 204 (2003)
11 Z. Yu, P.F. Barbara, J. Phys. Chem. B **108**, 11 321 (2004)
12 J.G. Müller, U. Lemmer, G. Raschke, M. Anni, U. Scherf, J.M. Lupton, J. Feldmann, Phys. Rev. Lett. **91**, 267 403 (2003)
13 C. Yin, C.Z. Yang, J. Appl. Polym. Sci. **82**, 263 (2001)
14 S.Y. Zhang, F. Kong, R. Sun, R.K. Yuan, X.Q. Jiang, C.Z. Yang, J. Appl. Polym. Sci. **89**, 2618 (2003)
15 B.E. Kohler, I.D.W. Samuel, J. Chem. Phys. **103**, 6248 (1995)
16 B.E. Kohler, J.C. Woehl, J. Chem. Phys. **103**, 6253 (1995)
17 S.N. Yaliraki, R.J. Silbey, J. Chem. Phys. **104**, 1245 (1996)
18 P. Papanek, J.E. Fischer, J.L. Sauvajol, A.J. Dianoux, G. Mao, M.J. Winokur, F.E. Karasz, Phys. Rev. B **50**, 15 668 (1994)
19 F. Kong, X.L. Wu, R.K. Yuan, C.Z. Yang, G.G. Siu, P.K. Chu, J. Vac. Sci. Technol. A **24**, 202 (2006)
20 C.J. Collison, L.J. Rothberg, V. Treemaneekarn, Y. Li, Macromolecules **34**, 2346 (2001)
21 T.Q. Nguyen, J. Wu, V. Doan, B.J. Schwartz, S.H. Tolbert, Science **288**, 652 (2000)
22 J.G. Müller, J.M. Lupton, J. Feldmann, U. Lemmer, U. Scherf, Appl. Phys. Lett. **84**, 1183 (2004)
23 H. Bassler, B. Schweitzer, Acc. Chem. Res. **32**, 173 (1999)
24 L.X. Chen, W.J.H. Jalger, M.P. Niemczyk, M.R. Wasielewski, J. Phys. Chem. A **103**, 4341 (1999)
25 L.D.A. Siebbeles, F.C. Grozema, M.P. de Haas, J.M. Warman, Radiat. Phys. Chem. **72**, 85 (2005)
26 F.C. Tsai, C.C. Chang, C.L. Liu, W.C. Chen, S.A. Jenekhe, Macromolecules **38**, 1958 (2005)
27 G. Rossi, R.R. Chanca, R. Silbey, J. Chem. Phys. **90**, 77 594 (1989)
28 A.K. Sheridan, J.M. Lupton, I.D.W. Samuel, D.D.C. Bradley, Synth. Met. **111–112**, 531 (2000)
29 A.R. Mantini, M.P. Marzocchi, G. Smulevich, J. Chem. Phys. **91**, 85 (1989)
30 T.G. Bjorklund, S.H. Lim, C.J. Bardeen, J. Phys. Chem. B **105**, 11 970 (2001)
31 G.D. Scholes, D.S. Larsen, G.R. Fleming, G. Rumbles, P.L. Burn, Phys. Rev. B **61**, 13 670 (2000)